Advances in Science and Technology Research Journal

Advances in Science and Technology Research Journal, 2025, 19(1), 256–268
https://doi.org/10.12913/22998624/195463
ISSN 2299-8624, License CC-BY 4.0

Received: 2024.09.09
Accepted: 2024.11.15
Published: 2024.12.01

The natural oscillations of perforated sifting surfaces with epicycloidal holes

Serhii Kharchenko[1*], Sylwester Samborski[2], Jakub Paśnik[3], Farida Kharchenko[4]

[1] Department of Applied Mechanics, Lublin University of Technology, ul. Nadbystrzycka 38D, 20-618 Lublin, Poland
[2] Department of Fundamentals of Production Engineering, Lublin University of Technology, ul. Nadbystrzycka 38D, 20-618 Lublin, Poland
[3] Department of Machine Design and Mechatronics, Lublin University of Technology, ul. Nadbystrzycka 38D, 20-618 Lublin, Poland
[4] Sumy National Agrarian University, 160 Herasyma Kondratieva Street, Sumy, 40000, Ukraine
* Corresponding author's e-mail: s.kharchenko@pollub.pl

ABSTRACT

The use of vibrational perforated sifting surfaces with holes of complex geometry provides intensive separation of loose materials by particle size and increases the technological efficiency of separating equipment. The lack of research methodologies and data on the oscillations of such perforated surfaces limits their application in practice, requires reliability studies and the derivation of appropriate patterns. The reliability analysis was conducted by studying the natural oscillation frequencies of perforated surfaces and checking for the absence of resonance phenomena. For the research, the methodology is based on numerical finite element methods in Abaqus_CAD and allows analyzing the natural oscillations of the structure when its structural parameters and boundary conditions are varied. To study the level of influence of the design of epicycloidal holes on the natural oscillations of perforated sifting surface, the identification of their values for round, epicycloidal (with a modulus of 5, 7 and 9) hole shapes was carried out. Patterns of variation in the natural oscillation frequencies of perforated surfaces are obtained depending on significant factors: surface thickness, hole spacing and epicycloid modulus. In addition, the analysis involved studying eight common modes of oscillation encountered in practice. The results were a research methodology, mathematical expressions for simplified calculation and analysis, patterns of oscillation changes of perforated sifting surfaces with holes of complex geometry. Studies enable the prediction of resonance phenomena and damage between the holes of perforated sifting surfaces, the absence of which determines their reliability.

Keywords: epicycloidal holes, perforated surface, oscillation frequency, design parameters, finite element method, resonance phenomena.

INTRODUCTION

The separation of loose material (LM) components by size is achieved using vibrating perforated sifting surfaces (PSS) on separating machines in various industries [1–3].

The efficiency of PSS depends on the following indicators: technological (productivity, completeness or clarity of separation) [4–5]; strength (oscillation frequency, reliability, wear resistance) [6], production (cost of resources during manufacture, payback) [7].

The use of holes in the shape of complex geometry allows to improve technological parameters (productivity and completeness of separation) [8–10]. The epicycloidal hole shape of PSS allows increasing the amount of sifted component (passage fraction) in comparison with PSS with basic round holes [8] or in the form of a regular triangle [10]. Application of three- and five-petal epicycloidal shapes of holes allowed to significantly intensify sifting of LM. Experimental studies have proved the intensity of loose materials sifting on PSS with Cassini oval holes compared to the elongated holes, at which the productivity increased by 15–20% [11].

Preliminary studies of the reliability of PSS with triangular and three-petal epicycloidal holes have shown a significant difference in their stress concentrators and durability [12]. Additionally, it is found that the natural oscillations frequency of PSS, which is necessary to exclude possible resonance phenomena, depends on the shape of holes of basic or complex geometry.

One of the most cost-effective methods today remains the production of PSS through cold stamping of sheet metal. Using dies and punch in presses, PSS are manufactured, during which the hole edges have technological and geometric deviations [13], and fatigue cracks [14]. The application of appropriate accounting for this effect in the numerical FE-model [15] has significantly reduced the calculation error to 5% and increased its adequacy.

The application of numerical studies for determining oscillation parameters, measuring stress concentrators and other strength indicators has shown its consistency in [12, 15, 16]. These methods have an advantage in accuracy and duration of studies compared to analytical and experimental methods. One common practice for validating the adequacy of numerical models of PSS, developed in Abaqus CAD, is to compare the results of FE-modeling with experiments conducted on the Simcenter Test Lab [13] or using the PSV-500 vibrometer [17].

This indicates the significance of the influence of the shape on the technological and strength parameters of PSS, their mass production. We can also conclude that the application of numerical modeling is promising for the identification of the natural oscillations of PSS with holes of complex geometry.

However, the prospects of PSS with holes of complex epicycloidal shape are insufficiently studied and require additional reliability studies. There is interest in the dependence of oscillation frequency of PSS on the epicycloid modulus (number of petals), which will avoid resonance phenomena and provide the necessary reliability.

The aim of the research is to determine the degree of parameters influence of PSS on the frequency of their natural oscillations depending on the parameters of holes of complex geometry using FE-modeling. The novelty of the work is to analyze the oscillation frequency of PSS with holes of complex geometry depending on the modulus (number of petals) of the epicycloid and to obtain the corresponding regularities

METHODOLOGY AND MATERIALS

For research, taking into account the data of previous works [13, 18] and existing studies [19, 20], we accept some conditions and assumptions:

1. The PSS is considered as a thin rectangular plate made of isotropic material.
2. The arrangement of holes with centers at the vertices of the hexagon, according to the practices of mass production.
3. We take as a basis the data obtained by numerically calculating the natural oscillation frequencies of PSS with round and epicycloidal holes with a modulus k = 5.
4. Variable parameters of PSS: surface thickness, epicycloid multiplicity, partition width.
5. Fix the dimensions of PSS: length 640 mm and width 260 mm.
6. PSS material: steel S235JR (yield strength 235 MPa; density 7.847 g/cm^3; Poisson's ratio 0.3).
7. Conditions for PSS fixing: all four edges are rigidly clamped.

One of the important technological parameters of PSS is the separating size of hole, relative to which the components of LM are separated. For a round hole of PSS this dimension is their diameter. For an epicycloidal hole – the diameter of the internal fixed circle, on the external surface of which the movable circle rolls over and forms an epicycloid. The ratio of the diameter of the fixed circle to the diameter of the movable circle forms the modulus of epicycloid (number of petals). Therefore, to study the influence of the hole shape on the oscillation frequencies of PSS, these diameters were the same.

Analysis of the works [12, 13, 21, 22] and preliminary studies [13, 18] showed a significant influence of PSS thickness and hole spacing (partition width) on the oscillation frequency variations. These parameters were also included in the research program.

We accept the following research algorithm:

1. Determining the geometric parameters of PSS for the research, and identify the significant factors.
2. Developing the numerical models of PSS with epicycloidal hole shapes, using modules k = 7

and $k = 9$, considering the accepted conditions and assumptions.
3. Conducting a comparative analysis of numerical models and determining the patterns of change in the natural oscillation frequencies of PSS based on their parameters.
4. Conducting an analysis of the geometric parameters of PSS holes and identifying patterns based on the epicycloid modulus and the natural oscillations frequency.
5. Developing scientific and technical recommendations for practical application.

We accept the following objects of study for rectangular PSS (Fig. 1): with round (basic) holes; with holes of complex geometry in the form of five-, seven-, and nine-petal epicycloids. An epicycloid is a curve that is formed by a moving circle with radius r relative to a stationary circle with radius R (Fig. 1). In this case, the separation dimension for dividing the components of LM is the hole diameter $d_s = 2R$. In the case of round holes, we also have $d_s = 2R$. There is a non-perforated (solid) part between the holes, which is denoted as partition width (a) and forms the stiffness of PSS structure. For round holes, this distance is measured between the circle edges with d_s, while for epicycloidal holes we have:

$$d_h = d_s + 2r = 2(R+r) \quad (1)$$

The epicycloid modulus can be conditionally determined in terms of the ratio $k = R/r$. Under the condition of fixing the separating hole size (i.e. R), the radius of the moving circle (i.e. r) will decrease as the modulus increases. This allows for maintaining the number of holes on PSS and its active sifting area. For convenience during the modeling process also used the value of the pitch between the hole centers (p), which was defined as: for round holes $p = 2R + a$; for epicycloidal holes $p = 2(R + r) + a$.

The significant factors and their levels of variation are presented in Table 1. The justification for the choice of these data and levels of variation is based on the results of preliminary studies, the experience of similar studies in this area [12, 13, 18, 21, 22]. The proposed epicycloidal holes require the formation of an appropriate classification according to the level of geometry complexity relative to regular shapes (in our case, a circle). It is necessary to take into account not only the geometry complexity of the hole itself but also their general arrangement per unit area of PSS.

The overall capacity of the perforated plate to sift LM components can be determined by the cross-sectional area (throughput) of PSS. Free area ratio (surface permeability) is defined as the ratio of the area of all holes to the area of PSS (Fig. 3):

$$k_p = \frac{S_p}{S_s} = \frac{n_h S_h}{S_s} \quad (2)$$

where: S_p – area of LM sifting through all holes of PSS; n_h – number (quantity) of holes on the test PSS, pieces; S_h – area of one hole, mm^2; S_s – total rectangular PSS area, mm^2.

For the studied surfaces, we have the following hole areas S_h:
− with basic round holes $S_{hc} = \pi R^2$;

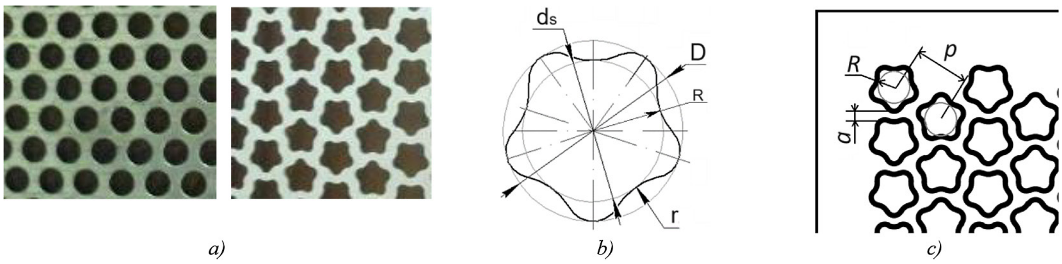

Figure 1. Prototypes of PSS: *a* – general view of PSS with round and five-petal epicycloid holes; *b* – schemes of PSS holes; *c* – schemes of PSS

Table 1. Significant factors and ranges of their variation

Level and range of factors variation	Factors		
	Partition width *a*, mm	Surface thickness *s*, mm	Epicycloid multiplicity *k*
+1	3	1.2	5
0	2	1	7
–1	1	0.8	9

- with holes of complex geometry in the form of an epicycloid were determined using the options of the Solid automatic design program.

The visualization of the sifting area of PSS with round and epicycloidal holes is shown in Figure 2. To account for the complexity of the hole geometry relative to the basic geometry (circle, rectangle, equilateral triangle), we introduce the corresponding geometry complexity coefficient K_{cg}. The value of this coefficient equals the ratio of the curve length, which forms a hole of complex geometry, to the circumference length of the basic round hole:

$$K_{cg} = L_{ep}/L_c \quad (3)$$

where: L_{ep} – length of the epicycloid curve (complex geometry hole); L_c – length of the circle (basic hole); $L_c = 2\pi R$.

The length of the epicycloid curve will depend on the values of the modulus and the corresponding radii of the fixed and moving circles. We divide the epicycloid curve into sections with convex and concave sectors, which have corresponding lengths l_1 and l_2 (Fig. 3). Then, the length of the epicycloid curve can be represented by the following expression:

$$L_{ep} = k(l_1 + l_2) \quad (4)$$

where: $l_1 = \frac{\pi r_1}{180}\alpha_1$, $l_2 = \frac{\pi r_2}{180}\alpha_2$ – lengths of the convex and concave curves, respectively (Fig. 3); r_1, r_2 – radii of the convex and concave curves, respectively; α_1, α_2 – the angles that define the boundaries of the convex and concave curves, respectively.

Taking into account the assumptions of expressions (3), (4), we have the final expression for determining the complexity coefficient of the hole geometry:

$$K_{cg} = (k\frac{\pi}{180}(r_1\alpha_1 + r_2\alpha_2))/2\pi R \quad (5)$$

Numerical modeling of PSS was performed in Simulia Abaqus, with its positive practice demonstrated in [13, 18]. The modeling was carried out according to the following algorithm (see Fig. 4): construct the geometry of the test PSS; input material properties; set calculation steps; define boundary conditions (fixing of PSS); generate the finite element mesh; create and initialize the task; visualize the calculations. In the Simulia Abaqus modeling, the following settings were used: quadrilateral first-order elements S4 and triangular elements S3; the linear model of elastic material; material characteristics: steel S235JR; the size of the final element – 1 mm; the total number of model elements – 164000 to 167000 FE. The

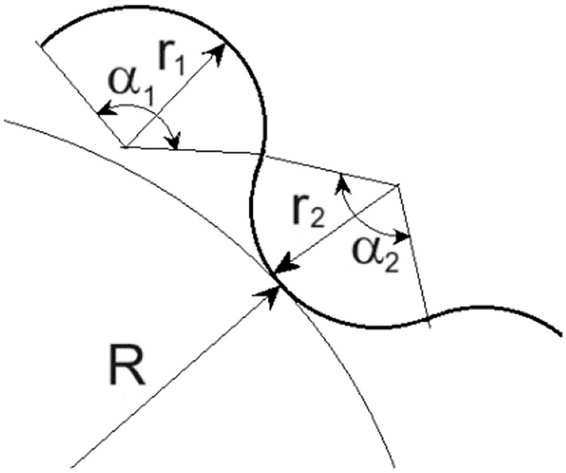

Figure 3. Scheme for determining the length of an epicycloid

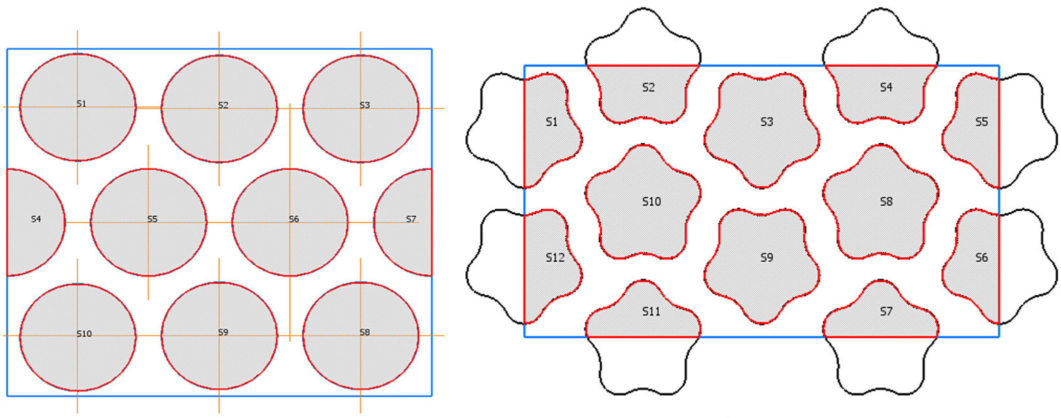

a) *b)*

Figure 2. Sifting area of LM through the holes of PSS (S_p): *a* – with round holes; *b* – with epicycloidal holes

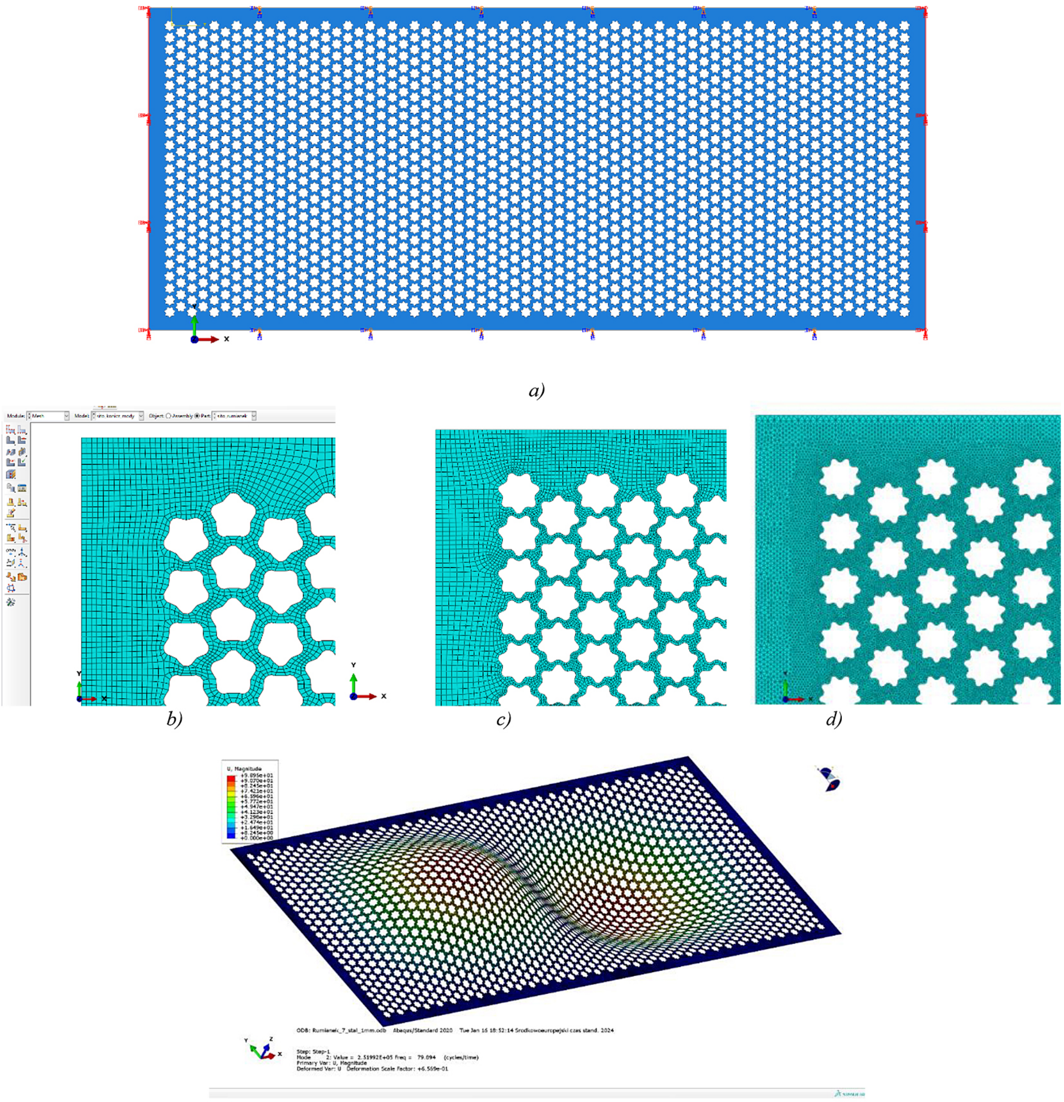

Figure 4. Some stages of numerical modeling of PSS: *a* – defining boundary conditions; *b, c, d* – constructing the finite element mesh of PSS with modules k = 5, k = 7, k = 9; *e* – visualizing the calculations

result of the modeling was data on the natural frequencies of PSS for different vibration modes.

RESEARCH RESULTS

As a result of the modeling, the natural frequencies of the experimental PSS (with round and epicycloidal holes) were obtained for the same modes (Tables 2–5, Figure 3).

The choice of these modes is explained by their potential practical use in the technological equipment of separation machines. However, if necessary, the developed methodology can also be used to identify the vibration parameters of the PSS under different conditions. The obtained patterns provide insight into the changes in the natural oscillations frequency, as well as potential resonance phenomena when using PSS with various types and parameters of holes. The trends in oscillation frequencies are similar with different modes.

It was also established that:

- an increase in the epicycloid modulus causes a decrease in the natural oscillations frequency of PSS by 0.2–3.7%;
- the natural oscillations frequency of PSS with epicycloidal holes exceeds 3.1% (at k = 5), 4.6% (at k = 7), and 1.9% (at k = 9) compared to the round holes;
- an increase in the surface thickness leads to an increase in the natural oscillations frequency by 32.17–32.37% (at k = 5), by 32.1–32.4% (at k = 7), and by 32.32–32.45% (at k = 9);

Table 2. Visual representation of the vibration modes of the experimental PSS

Mode	Visual images	Mode	Visual images
1	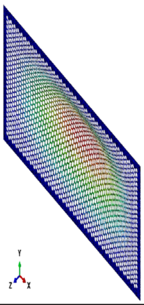	5	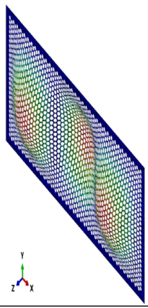
2	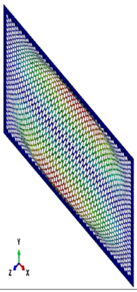	6	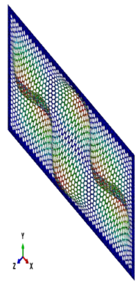
3	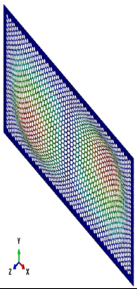	7	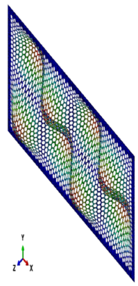
4	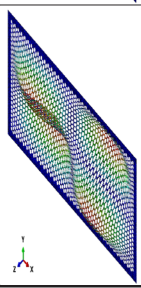	8	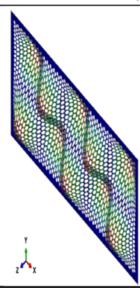

Table 3. Dependence of the natural oscillations frequency steel PSS with holes of complex geometry on the plate thickness and the partition width between the holes (k = 5)*

Mode	Partition width between the holes *a* = 1 mm			Partition width between the holes *a* = 2 mm			Partition width between the holes *a* = 3 mm		
	Thickness *s*, mm			Thickness *s*, mm			Thickness *s*, mm		
	0.8	1.0	1.2	0.8	1.0	1.2	0.8	1.0	1.2
1	53.19	65.05	76.36	55.86	69.32	82.57	56.82	70.70	84.46
2	141.17	172.66	202.71	147.94	183.62	218.76	150.31	187.03	223.43
3	61.98	75.82	89.02	65.44	81.17	96.62	66.86	83.20	99.38
4	150.21	183.70	215.66	157.79	195.78	233.13	160.58	199.81	238.67
5	78.14	95.63	112.36	82.96	102.86	122.41	85.25	106.06	126.69
6	165.72	202.65	237.86	174.73	216.68	257.90	178.25	221.78	264.90
7	188.21	230.19	270.23	199.11	243.83	293.66	203.76	253.49	302.76
8	217.92	266.60	313.06	231.24	286.59	340.90	237.37	295.30	352.68

Note: * research results from [18].

Table 4. Dependence of the natural oscillations frequency steel PSS on the plate thickness and the partition width between the holes (k = 7)

Moda	Partition width between the holes *a* = 1 mm			Partition width between the holes *a* = 2 mm			Partition width between the holes *a* = 3 mm		
	Thickness *s*, mm			Thickness *s*, mm			Thickness *s*, mm		
	0.8	1.0	1.2	0.8	1.0	1.2	0.8	1.0	1.2
1	52.42	64.41	75.97	55.33	68.68	81.83	57.88	72.04	86.09
2	139.34	171.29	202.15	146.75	182.17	217.11	152.89	190.32	227.44
3	60.42	74.09	87.23	64.43	79.89	95.11	67.69	84.23	100.62
4	147.69	181.36	213.80	156.17	193.77	230.81	163.02	202.89	242.42
5	75.10	91.95	108.08	81.05	100.44	119.48	85.62	106.52	127.21
6	161.97	198.61	233.78	172.32	213.68	254.34	180.39	224.46	268.13
7	182.60	223.62	262.89	195.60	242.41	288.36	205.43	255.56	305.21
8	209.83	256.73	301.53	226.24	280.28	333.27	238.40	296.52	354.06

Table 5. Dependence of the natural oscillations frequency steel PSS on the plate thickness and the partition width between the holes (k = 9)

Moda	Partition width between the holes *a* = 1 mm			Partition width between the holes *a* = 2 mm			Partition width between the holes *a* = 3 mm		
	Thickness *s*, mm			Thickness *s*, mm			Thickness *s*, mm		
	0.8	1.0	1.2	0.8	1.0	1.2	0.8	1.0	1.2
1	52.01	64.31	76.27	54.29	67.41	80.37	55.64	69.23	82.70
2	138.31	170.86	202.71	143.91	178.68	213.03	147.40	183.39	219.07
3	60.36	74.41	88.08	63.60	78.94	94.07	65.55	81.55	97.40
4	146.89	181.29	214.88	153.51	190.56	227.15	157.57	196.03	234.15
5	75.55	92,99	109.91	80,62	100.03	119.18	83.66	104.05	124.27
6	161.61	199.22	235.84	169,98	210.96	251.39	175.02	217.70	260.01
7	182.88	225.19	266.27	193,73	240.38	286.39	200.17	248.97	297.32
8	210.92	259.49	306.55	225.01	279.15	332.51	233.29	290.13	346.44

Table 6. Dependence of the natural oscillation frequency steel PSS on the plate thickness and the epicycloid modulus (a = 2 mm, R = 3.5 mm)

Moda	PSS with holes of complex geometry k = 5*			PSS with holes of complex geometry k = 7			PSS with holes of complex geometry k = 9			PSS with round holes (ds = 7 mm)*		
	Thickness *s*, mm			Thickness *s*, mm			Thickness *s*, mm			Thickness *s*, mm		
	0.8	1.0	1.2	0.8	1.0	1.2	0.8	1.0	1.2	0.8	1.0	1.2
1	55.86	69.32	82.57	55.33	68.68	81.83	54.29	67.41	80.37	54.11	67.20	80.11
2	147.94	183.62	218.76	146.75	182.17	217.11	143.91	178.68	213.03	143.86	178.65	212.96
3	65.44	81.17	96.62	64.43	79.89	95.11	63.60	78.94	94.07	64.21	79.73	95.04
4	157.79	195.78	233.13	156.17	193.77	230.81	153.51	190.56	227.15	154.16	191.43	228.19
5	82.96	102.86	122.41	81.05	100.44	119.48	80.62	100.03	119.18	82.62	102.58	122.27
6	174.73	216.68	257.90	172.32	213.68	254.34	169.98	210.96	251.39	171.89	213.43	254.39
7	199.11	243.83	293.66	195.60	242.41	288.36	193.73	240.38	286.39	197.43	245.12	292.15
8	231.24	286.59	340.90	226.24	280.28	333.27	225.01	279.15	332.51	231.04	286.83	341.83

Note: * research results from [18].

- increasing the partition width between holes leads to an increase in the natural oscillations frequency by 7.7–9.8% (at k = 5), by 10–13.7% (at k = 7), and by 7.5–10.6% (at k = 9).

One of the tasks set was to rank factors based on their significance. It was found that the PSS thickness has the maximum impact (up to 32.45%), the average impact has partition width

Table 7. Dependence of the natural oscillation frequency steel PSS on the partition width between the holes and the epicycloid modulus (s = 1 mm; R = 3.5 mm)

Moda	PSS with holes of complex geometry k = 5*			PSS with holes of complex geometry k = 7			PSS with holes of complex geometry k = 9			PSS with round holes (ds = 7 mm)*		
	Partition width between holes *a*, mm			Partition width between holes *a*, mm			Partition width between holes *a*, mm			Partition width between holes *a*, mm		
	1	2	3	1	2	3	1	2	3	1	2	3
1	65.05	69.32	70.70	64.41	68.68	72.04	64.31	67.41	69.23	63.11	67.20	68.72
2	172.66	183.62	187.03	171.29	182.17	190.32	170.86	178.68	183.39	167.85	178.65	182.59
3	75.82	81.17	83.20	74.09	79.89	84.23	74.41	78.94	81.55	74.64	79.73	81.76
4	183.70	195.78	199.81	181.36	193.77	202.89	181.29	190.56	196.03	179.69	191.43	195.93
5	95.63	102.86	106.06	91.95	100.44	106.52	92.99	100.03	104.05	95.71	102.58	105.53
6	202.65	216.68	221.78	198.61	213.68	224.46	199.22	210.96	217.70	199.99	213.43	218.81
7	230.19	243.83	253.49	223.62	242.41	255.56	225.19	240.38	248.97	229.27	245.12	251.77
8	266.60	286.59	295.30	256.73	280.28	296.52	259.49	279.15	290.13	267.83	286.83	295.11

Note: * research results from [18].

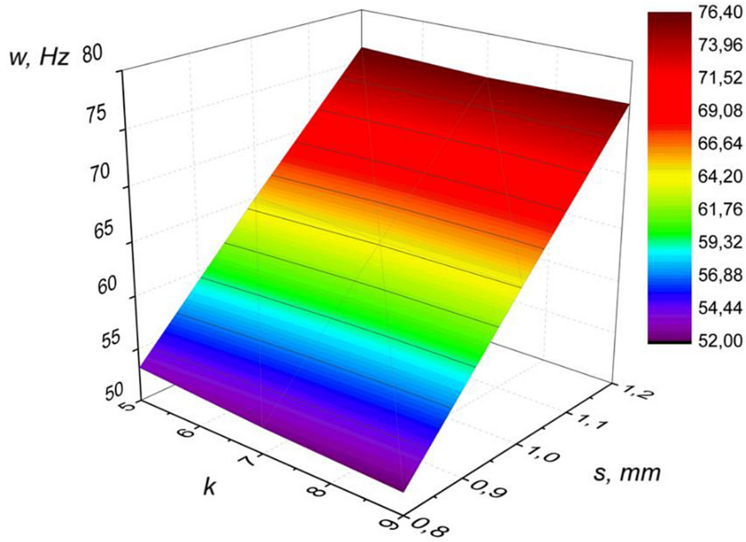

Figure 5. Dependencies of the natural frequencies of the perforated plates on the surface thickness and the modulus of the epicycloid in 3D: mode_1, a = 1 mm

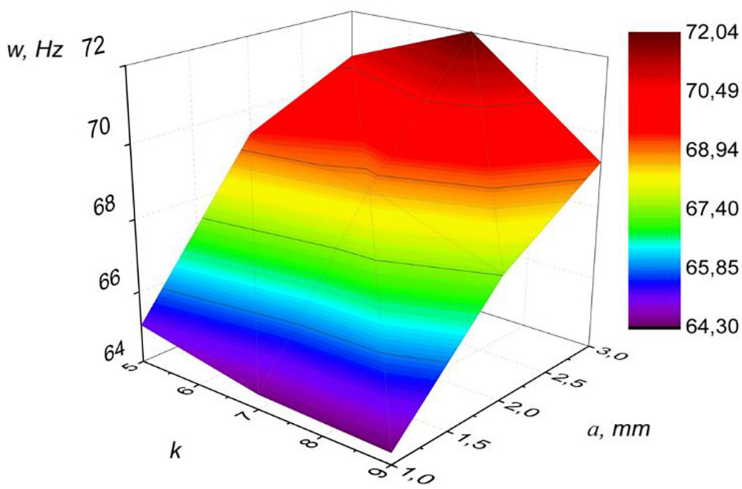

Figure 6. Dependencies of the natural frequencies of the perforated plates on the modulus of the epicycloid and partition width between holes: mode_1, s = 1 mm

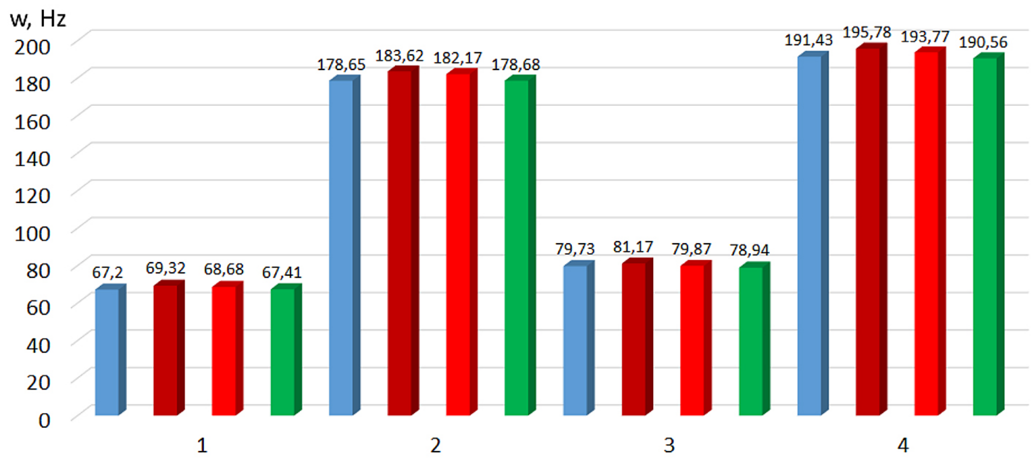

Figure 7. The natural oscillation frequencies of PSS under different modes (1–8): – k = 0 (round holes); – k = 5; – k = 7; – k = 9

between holes (up to 13.7%) and the smallest impact belongs to the epicycloid modulus (up to 3.7%). The next stage of the research involved a comprehensive linking of geometric parameters to the frequency characteristics of PSS.

Using expression (2), the free area ratio (surface permeability) k_p was determined (Table 8, Fig. 8), and using expression (5), the value of the geometry complexity coefficient of the hole was established (Table 9, Fig. 9).

The use of coefficient K_{sg} allows analyzing the level of complexity of the hole geometry through the length of the curve that forms it. For example, the use of such a coefficient will be appropriate for a comparative analysis of PSS with different shapes of holes in the form of: epicycloid, hexagon, Cassini oval, epitrochoid, etc.

ANALYSIS AND DISCUSSION OF RESULTS

After obtaining the main (Fig. 5–7) and additional (Fig. 8, 9) dependencies, it is necessary to integrate them. Such a combination will enhance the capabilities of systematic analysis and practical application of the results. The obtained dependencies of the natural oscillation frequencies of PSS on the free area ratio and the complexity coefficient of the hole (Fig. 10, 11) at different epicycloid modules were established.

Approximation of the data allowed us to obtain the corresponding equations:

a) for mode 1 (Fig. 10) we have:

- at k = 5 $y = 87.669e^{-0,386x}$ $R^2 = 0.9922$;
- at k = 7 $y = 94.293e^{-0,531x}$ $R^2 = 0.9875$;
- at k = 9 $y = 84.662e^{-0,4x}$ $R^2 = 0.9915$;

Table 8. Geometric parameters and values of the free area ratio (surface permeability k_p) for the tested PSS, (ds = 7 mm, D = 9 mm, S_s, mm²)

k	*a*, mm	*L*, curve length, mm	S_p, mm²	k_p
0 (round base)	1	21.99	389.98	0.75
	2		325.74	0.63
	3		257.29	0.50
5	1	27.74	400.19	0.77
	2		320.91	0.62
	3		284.23	0.55
7	1	30.01	367.16	0.71
	2		318.25	0.61
	3		261.36	0.50
9	1	32.96	356.11	0.69
	2		290.58	0.56
	3		261.82	0.51

Table 9. Geometric parameters and values of the geometry complexity coefficient of the hole of PSS, (ds = 7 mm, D = 9 mm)

k	r_1, mm	r_2, mm	L_{ep}, mm	L_c, mm	K_{cg}
0	-	-	21.99	21.99	1
5	1.5	2.35	27.74		1.26
7	0.94	1.23	30.01		1.36
9	0.68	0.83	32.96		1.5

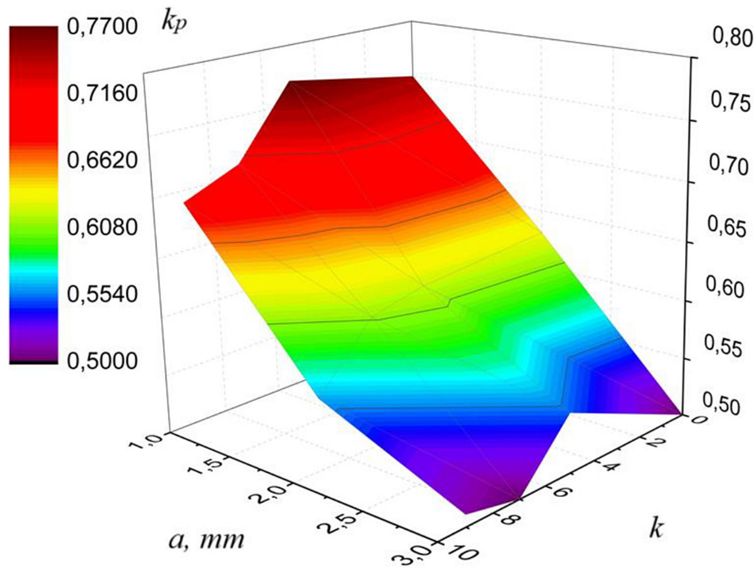

Figure 8. Change in free area ratio of the perforated plate depending on the modulus of the epicycloid and partition width between holes

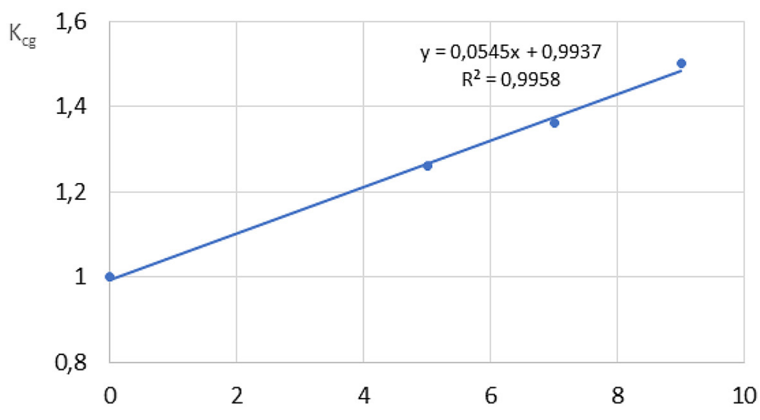

Figure 9. Change in the geometric complexity coefficient of the hole of PSS depending on the epicycloid modulus

− at k = 0 $y = 81.899e^{-0,339x}$ $R^2 = 0.9357$;

b) for mode 3 (Fig. 11) we have:

− at k = 5 $y = 87.669e^{-0,386x}$ $R^2 = 0.9922$;

− at k = 7 $y = 94.293e^{-0,531x}$ $R^2 = 0.9875$;

− at k = 9 $y = 84.662e^{-0,4x}$ $R^2 = 0.9915$;

− at k = 0 $y = 81.899e^{-0,339x}$ $R^2 = 0.9357$.

These dependencies give an idea of the changes in frequency characteristics depending on other possible values of the parameters of holes of complex geometry. Thus, despite the established oscillation parameters, it is possible to investigate the parameters for PSS with other epicycloidal modules, surface thickness, or hole spacing.

One of the main tasks we set ourselves was to develop a methodology for identifying the natural oscillations of perforated surfaces with holes

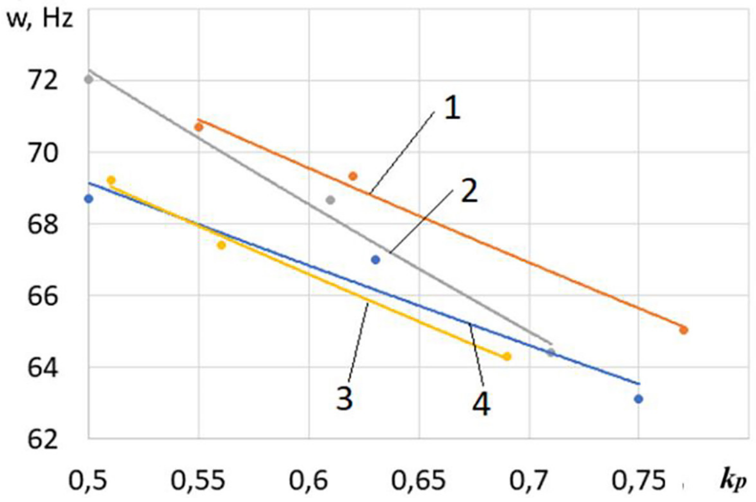

Figure 10. The natural oscillation frequencies of PSS depending on the free area ratio and the epicycloid modulus (mode №1, *s* = 1 mm): 1 – *k* = 5; 2 – *k* = 7; 3 – *k* = 9; 4 – *k* = 0 (round holes)

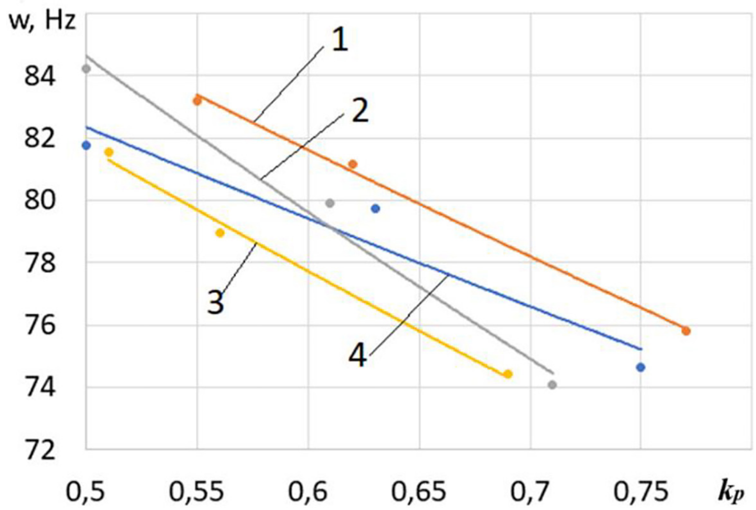

Figure 11. The natural oscillation frequencies of PSS depending on the free area ratio and the epicycloid modulus (mode 3, s = 1 mm): 1 – *k* = 5; 2 – *k* = 7; 3 – *k* = 9; 4 – *k* = 0 (round holes)

of complex geometry. This methodology can be used for studies with other parameters, including material. In one of our other papers, we studied and compared the natural frequencies of perforated plates made of steel and aluminium [23]. Of course, we obtained different values, but the trend of changes remained constant (in relation to the vibration modes). If necessary, you can use correction factors to correct the results that may occur when changing the material.

The wide range of applications of sifting surfaces in various technologies results in a significant amount of different kinematic parameters in serial separation equipment. The value of the amplitude and frequency of forced oscillations is optimised depending on the properties of the loose material. Therefore, it is difficult to make a comparison with a specific type of serial separation equipment. For this reason, we have identified the natural oscillation frequencies for the different eight modes, which will allow us to take into account all variants of serial separation equipment.

The developed methodology and obtained data create the opportunity for research and design of PSS with high reliability, sifting capacity, and economic profitability in their production.

Among the prospects of using the methodology, in particular, the integration of geometric parameters for system evaluation, is the potential possibility of analysis in terms of the criteria of stress concentrators and separation efficiency.

CONCLUSIONS

As a result of the research, a method for determining the influence of parameters by holes of complex geometry on the frequency characteristics of PSS, which is based on numerical FE-modeling. Adequate conditions are obtained for modeling the frequency characteristics of PSS with holes of complex geometry in the Abaqus CAD program. To study the level of influence of the design of epicycloidal holes on the natural oscillations of PSS, the identification of their values for round, epicycloidal (with a modulus of 5, 7 and 9) hole shapes was carried out. This also allowed us to determine the natural frequencies of PSS while varying parameters such as the epicycloid module, distance between holes, surface thickness, and to assess the significance levels of these factors. In addition, the analysis involved studying eight common modes of oscillation encountered in practice.

For a comprehensive analysis and practical application, new coefficients have been introduced that account for the structural parameters of the holes – the complexity coefficient of the hole of the entire PSS – the free area ratio.

The established dependencies of the natural oscillation frequencies of PSS on these coefficients allow for assessing trends and making predictions.

The conducted research, through the developed methodology and established results, allows for the optimization of the structural-kinematic parameters of PSS with holes of complex geometry at the stages of their research, design, manufacturing, and operation. Studies enable the prediction of resonance phenomena and damage between the holes of perforated sifting surfaces, the absence of which determines their reliability.

Acknowledgments

The authors acknowledge the financial support of the National Science Centre in Krakow to the research project funded in the „POLONEZ BIS 2» call No. 2022/45/P/ST8/02312 entitled Numerical-experimental analysis of a sieve holes' shape and arrangement effect on the degree. POLONEZ BIS is operated by the Centre on the basis of the Grant Agreement No. 945339 concluded with the European Research Executive Agency.

REFERENCES

1. Liu H, Jia J, Liu N, Hu X, Zhou X. Effect of material feed rate on sieving performance of vibrating screen for batch mixing equipment. Powder Technology 2018; 338: 898–904, https://doi.org/10.1016/j.powtec.2018.07.046
2. Hou J, Liu X, Zhu H, Ma Z, Tang Z, Yu Y, Jin J, Wang W. Design and motion process of air-sieve castor cleaning device based on discrete element method. *Agriculture* 2023; *13*: 1130, https://doi.org/10.3390/agriculture13061130
3. Jesny S, Prasobh G. A review on size separation. International Journal of Pharmaceutical Research and Applications 2022; 7(2): 286–296, https://doi.org/10.35629/7781-0702286296
4. Tishchenko L, Kharchenko S, Kharchenko F, Bredykhin V, Tsurkan O. Identification of a mixture of grain particle velocity through the holes of the vibrating sieves grain separators. East. Eur. J. Enterp. Technol. 2016, 2: 63–69. https://doi.org/10.15587/1729-4061.2016.65920
5. Kaliramesh S, Kingsly A. Predicting particle separation and sieve blinding during wheat flour sifting. Transactions of the ASABE 2021; 64: 1103-1112. https://doi.org/10.13031/trans.14276
6. Andh UB, Chavan SM and Kulakrni SG. Stress analysis of perforated plates under uniaxial compression using experimentation and finite element analysis. International Journal of Current Engineering and Technology 2017; 7(2): 431–437.
7. Wang W, Zhu D, Allen D, Almondb H. Non-traditional machining techniques for fabricating metal aerospace filters. Chin. J. Aeronaut. 2008; 21: 441–447.
8. Kharchenko S, Kovalyshyn S, Zavgorodniy A, Kharchenko F, Mikhaylov Y. Effective sifting of flat seeds through sieve. INMATEH-Agricultural Engineering 2019; 58(2): 17–26. https://doi.org/10.35633/INMATEH-58-02
9. Bakum M, Kharchenko S, Kovalyshyn S, Krekot M, Kharchenko F, Shvets O, Kiełbasa P, Miernik A. Identification of parameters of the separation process of safflower seed material on sieves. Journal of Physics: Conference Series 2022, 2408, 012013 IOP Publishing, https://doi.org/10.1088/1742-6596/2408/1/012013
10. Kharchenko S. Intensification of grain sifting on flat sieves of vibration grain separators: monograph; Dissa Plus: Kharkiv, 2017; 217.
11. Bredykhin V, Tikunov S, Slipchenko M, Aifyorov O, Bogomolov A, Shchur T, Kocira S, Kiczorowski P, Paslavskyy R. Improving efficiency of corn seed separation and calibration process. Sciendo. Agricultural Engineering 2023; 27(1): 241–253, https://doi.org/10.2478/agriceng-2023-0018

12. Kharchenko S, Samborski S, Kharchenko F, Paśnik J, Kovalyshyn S, Sirovitskiy K. Influence of physical and constructive parameters on durability of sieves of grain cleaning machines. Advances in Science and Technology Research Journal 2022; 16(6): 156–165.
13. Kharchenko S, Samborski S, Kharchenko F, Mitura A, Paśnik J, Korzec I. Identification of the natural frequencies of oscillations of perforated vibrosurfaces with holes of complex geometry. Materials 2023; 16: 5735, https://doi.org/10.3390/ma16175735
14. Thomas D. Effect of mechanical cut-edges on the fatigue and formability performance of advanced high-strength steels. J. Fail. Anal. and Preven. 2012; 12: 518–531, https://doi.org/10.1007/s11668-012-9591-z
15. Jayavardhan HK, Samal PK. Effect of Shape of Cut-out on Natural Frequency of Square Plate. IOP Conf. Series: Materials Science and Engineering 2021; 1189(2021): 012028, https://doi.org/10.1088/1757-899X/1189/1/012028
16. Pavan Kishore ML, Rajesh CH, Komawar R. Free vibrational characteristics determination of plates with various cutouts. Vibroengineering Procedia 2019; 22. https://doi.org/10.21595/vp.2018.20286.
17. Kharchenko S, Samborski S, Kharchenko F, Paśnik J, Korzec I, Mitura A, Kłoda Ł. Numerical study of the natural oscillations of perforated vibrating surfaces with holes of complex geometry. VIII International Conference of Computational Methods in Engineering Science - CMES 2023 (Puławy, Poland, 23.11–25.11. 2023). Polish Air Force University Dęblin, 2023; 78.
18. Kharchenko S, Samborski S, Kharchenko F, Kotliarevskyi I. Determination of hole blocking conditions for perforated sifting surfaces. ASTRJ. 2024; 18(5): 342–360. https://doi.org/10.12913/22998624/190483
19. Jhung M, Jeong K. Free vibration analysis of perforated plate with square penetration pattern using equivalent material properties, Nuclear Engineering and Technology 2015; 47(4): 500–511, https://doi.org/10.1016/j.net.2015.01.012
20. Israr A. *Vibration analysis of cracked aluminium plates.* PhD thesis, University of Glasgow 2008; 181.
21. Torabi K, Azadi A. Vibration analysis for rectangular plate having a circular central hole with point support by Rayleigh-Ritz Method. Journal of Solid Mechanics 2014; 6(1): 28–42.
22. Kharchenko S, Samborski S, Kharchenko F. Intensification of technological processes of equipment for post-harvest processing of grain. Study of reliability of sieves with complex shapes of holes. 1 st Workshop on Experimental and Computational Mechanics "WECM'22" + DIACMEC Lublin, Poland, June 1st 2022; 12.
23. Kharchenko S, Samborski S, Kharchenko F, Paśnik J. numerical study of the natural oscillations of perforated vibrating surfaces with holes of complex geometry. Advances in Science and Technology Research Journal. 2023; 17(6): 73–87. https://doi.org/10.12913/22998624/174062